Turk J Phys
28 (2004) , 139 – 144.

Design and Preparation of Antireflection and Reflection Optical Coatings

Özlem DUYAR, Hüseyin Zafer DURUSOY*
Department of Physics Engineering, Hacettepe University,
Beytepe, 06532 Ankara-TURKEY
e-mail: hzd@hacettepe.edu.tr

Received 11.02.2003

Abstract

In this study, reflective and antireflective coatings were designed and simulated. Optical transmission and reflection values were deduced with a matrix formulation via a personal computer.

It was found that the number of layers affects the optical performance. The width of the high-reflectance region in the reflectance curves decreases, while its height increases with the increasing number of layers for the reflective coating design. The antireflection coatings transmit about 99.89% in a broad high-pass band at the central wavelength of $\lambda_0 = 450$ nm. In addition, simulated Fabry-Perot filters result in a single sharp transmittance peak at the desired central wavelength. The half-width of the transmission band at central wavelength decreases and its peak height increases with the increasing number of the coated layers.

To compare with theory, both sides of a glass substrate were deposited a two-layer coating of MgO/MgF_2 via electron beam evaporation, to produce an antireflective coatings in the visible and near infrared regions. The optical properties of prepared films were studied through optical transmission measurements. The peak transmittance was 98.2% at the central wavelength $\lambda_\circ = 450\ nm$.

Key Words: Optical coating, Antireflective coating, Reflective coating, Optical properties.

1. Introduction

Reflective and antireflective (AR) optical coatings have long been developed for a variety of applications in all aspects of use; for optical and electro-optical systems in telecommunications, medicine, military products and consumer products. AR coatings have been widely used in many applications including glass lenses, eyeglasses, lasers, mirrors, solar cells, IR diodes, multipurpose broad and narrow band-pass filters, architectural and automotive glass and displays such as cathode ray tubes, as well as plasma, liquid crystal and flat panel displays. In addition, highly reflecting dielectric mirrors have been developed to be used in gas lasers and in Fabry-Perot interferometers [1–10].

E-beam evaporation is the preferred deposition method for large-scale applications. However, magnetron sputtering techniques provide good uniformity for smaller area coatings [8–13]. Presently, the use of ion-assisted and laser ablation deposition techniques in preparation of optical coatings have been the subject of research and development [14]. This study reports the design and simulation of the reflective and antireflective multilayer optical coatings as well as results of some experimental studies.

*Corresponding author

2. Theory

The optical matrix approach was employed for N-layer design of antireflection and reflection coatings. The main idea of this method is matching the E- and H-fields of the incident light on the interfaces of multilayer optical coatings. The matrix relation defining the N-layer antireflection coating problem is given by [3]

$$\begin{bmatrix} B \\ C \end{bmatrix} = \left\{ \prod_{j=1}^{N} \begin{bmatrix} \cos\delta_j & \frac{i\sin\delta_j}{\eta_j} \\ i\eta_j \sin\delta_j & \cos\delta_j \end{bmatrix} \right\} \begin{bmatrix} 1 \\ \eta_{sub} \end{bmatrix}, \tag{1}$$

where B and C are total electric and magnetic field amplitudes of the light propagating in the medium. Thus optical admittance is given by the ratio

$$Y = \frac{C}{B}. \tag{2}$$

The following relations give reflectance, transmittance and absorbance, respectively:

$$R = \left(\frac{n_0 - Y}{n_0 + Y}\right)\left(\frac{n_0 - Y}{n_0 + Y}\right)^* \tag{3}$$

$$T = \frac{4y_0 Re(y_{sub})}{(y_0 B + C)\,(y_0 B + C)^*} \tag{4}$$

$$A = 1 - T - R = (1 - R)\left(1 - \frac{Re(\eta_s)}{Re(BC^*)}\right). \tag{5}$$

Thus, each layer is represented by a 2×2 matrix M, of the form

$$M_j = \begin{bmatrix} \cos\delta_j & \frac{i\sin\delta_j}{\eta_j} \\ i\eta_j \sin\delta_j & \cos\delta_j \end{bmatrix}, \tag{6}$$

where $\eta_p = y_j/\cos\theta$ for p-polarization, $\eta_s = y_j \cos\theta$ for s-polarization, $\delta_j = [2\pi(n_j - ik_j)d_j \cos\theta_j]/\lambda$, $n_\circ \sin\theta_\circ = n_j \sin\theta_j$ and δ_j, y_j, n_j, d_j, θ_j and λ are the optical phase shift, optical admittance, refractive index, physical thickness, incident angle, and light beam wavelength, respectively, of the homogenous j^{th} thin film layer. These expressions are obtained by replacing all y's by η's and multiplying all δ's by an appropriate $\cos\theta$. For oblique incidence $\theta = 0$ and $\cos\theta = 1$.

The order of high and low indices of film layers is a crucial parameter for designing highly antireflective or highly reflective optical coatings. The correct index order is: air (a) | low index (L) | high index (H) | substrate (s) for antireflection coatings by using a superlattice of double-layer, quarter-wave-thickness films. This index order is reversed for the design of highly reflecting coatings. The reflectance and transmittance curves can be calculated with the optical matrix theory presented above for as many layers as desired.

The reflectance curves in the 350–600 nm visible region of electromagnetic spectrum for $N = 2$, $N = 3$, $N = 7$ and $N = 11$ layers have been simulated and plotted in Figure 1. These periodic structures of alternately high and low index materials can be designed by s | $(HL)^m$ | a for highly reflective coatings. The maximum reflectance of these structures can be increased with the insertion of an extra H layer between the low index material and the incident medium, so that it has the form s | $(HL)^m$ H | a. Quartz glasses

were taken as substrates for simulation of multilayer films. TiO_2 ($n = 2.42$) and MgF_2 ($n = 1.38$) were selected as the high refractive index and low refractive index materials at the central wavelength $\lambda_0 = 450$ nm, respectively. With the increasing number of layers, the width of the high-reflectance region in these curves decreases while its height increases, as shown in the Figure 1. The reflectance rapidly approaches to 100% by increasing the number of layers.

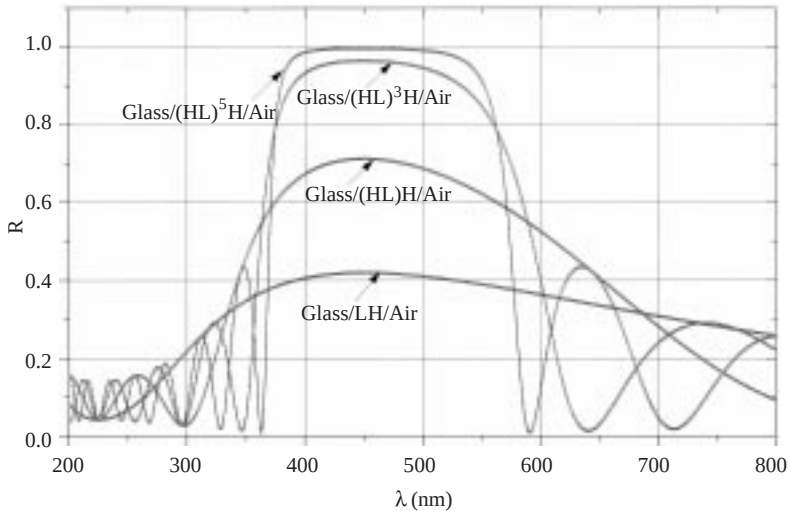

Figure 1. Simulated reflectance of a high-low index stack for (a) $N = 2$, (b) $N = 3$, (c) $N = 7$, (d) $N = 11$. Layers are $\lambda/4$ thick at $\lambda_0 = 450$ nm. In all cases, $n_H = 2.42$, $n_L = 1.38$, $n_S = 1.52$ and $n_0 = 1.00$.

Figure 2 shows the simulated transmittance curves for the $N = 4$ and $N = 8$ layers for broad band antireflection coatings at the central wavelength, $\lambda_0 = 450$ nm. While these coatings transmit about 99.9% in a broad high pass band, the uncoated glass would only transmit about 91.4% of the incident light as illustrated in Figure 2.

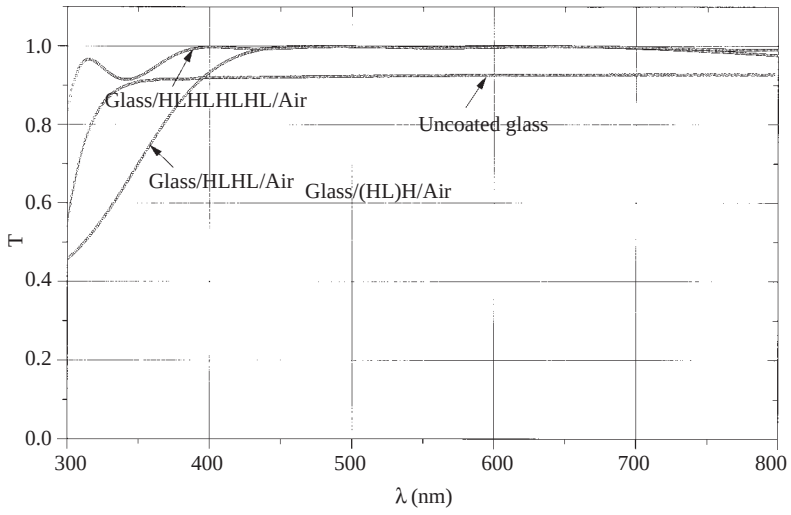

Figure 2. Simulated transmittance for several periodic structures at $\lambda_0 = 450$ nm: (a) s|HLHL|a, (b) s|HLHLHLHL|a. In all cases, $n_H = 2.42$, $n_L = 1.38$, $n_S = 1.52$ and $n_0 = 1.00$.

Design of narrow band pass filters or the Fabry-Perot filters results in a single sharp transmittance peak. Two possible examples of Fabry-Perot filters s | HLH LL HLH | a and s | HLHL HH LHLH | a have been

studied. Thickness of the central double layer is half-wavelength thick. The transmittance curves have been calculated and plotted in Figure 3 for dielectric materials TiO_2, MgF_2 of the type s | HLH LL HLH | a and s | HLHL HH LHLH | a. The half-width of the transmission band at central wavelength $\lambda_0 = 450$ nm decreases and its peak height increases with the number of the coated layers as illustrated in this figure. As the number of layers was further increased, the side peaks would be suppressed.

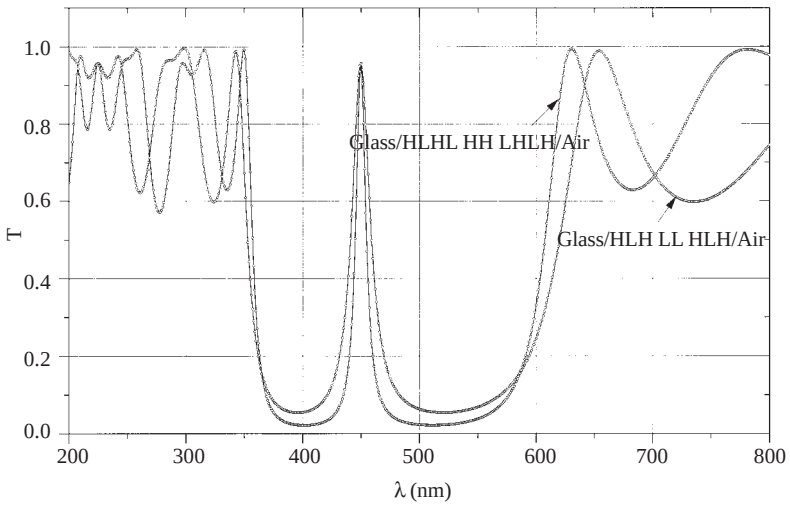

Figure3. Simulated transmittance of the various dielectric Fabry-Perot filters: (a) s|HLH LL HLH|a, (b) s|HLHL HH LHLH|a. In all cases, $n_H = 2.42$, $n_L = 1.38$, $n_S = 1.52$ and $n_0 = 1.00$.

3. Comparison with Experiment

In order to compare our simulations with experiments, we calculated and plotted the transmittance of a double-layer antireflection coating MgO/MgF_2on glass substrate in the visible region of the electromagnetic spectrum. Transmission spectra of the optical coatings were measured with a Varian Carry 5E spectrophotometer in the range of 300 nm to 1500 nm. The measured curve (shown in Figure 4) shows very good agreement between the theoretical and experimental results. The refractive index of the coating materials were assumed to be independent of the wavelength and they were assumed to be nonabsorbing materials (k = 0) to simplify the theoretical calculations.

According to the double layer AR coating theory for nonabsorbing films and for normal incidence of light, the matrix equation becomes [3],

$$\begin{bmatrix} B \\ C \end{bmatrix} = \begin{bmatrix} \cos\delta_1 & \frac{i\sin\delta_1}{\eta_1} \\ i\eta_1\sin\delta_1 & \cos\delta_1 \end{bmatrix} \begin{bmatrix} \cos\delta_2 & \frac{i\sin\delta_2}{\eta_2} \\ i\eta_2\sin\delta_2 & \cos\delta_2 \end{bmatrix} \begin{bmatrix} 1 \\ \eta_s \end{bmatrix}. \tag{7}$$

Thus, admittance is given by

$$Y = \frac{i\eta_1\sin\delta_1(\cos\delta_2 + i\frac{\eta_s}{\eta_2}\sin\delta_2) + \cos\delta_1(\eta_s\cos\delta_2 + i\eta_2\sin\delta_2)}{\cos\delta_1(\cos\delta_2 + i\frac{\eta_s}{\eta_2}\sin\delta_2) + \frac{i\sin\delta_1}{\eta_1}(\eta_s\cos\delta_2 + i\eta_2\sin\delta_2)}. \tag{8}$$

Then the reflectance for a double layer of quarter wave thickness at normal incidence as a result of [2] and [8] is given by

$$R = \left(\frac{\eta_0\eta_2^2 - \eta_S\eta_1^2}{\eta_0\eta_2^2 + \eta_S\eta_1^2}\right)^2.$$

The reflectance is reduced to zero for incidence of light from air ($\eta_0 = 1$) when $\sqrt{n_s} = n_2/n_1$, where n_s, n_1 and n_2 are the refractive indices of substrate, bottom coating, and top coating, respectively. The optical thicknesses of the layers were taken as a quarter wavelength $d = \lambda_0/4n$ for the reflected waves to interfere destructively, where λ_0 is the central wavelength. As for the antireflection coating materials, we chose MgO ($n = 1.65$) as the high refractive index material and MgF_2(n = 1.38) as the low refractive index material at the central wavelength $\lambda_0 = 450$ nm. MgF_2 in combination with high refractive index oxide materials is widely used in the design of antireflection coatings. Thus, we decided that MgO is a convenient material to deposite on MgF_2 for narrow band coating in the visible region according to the two layer antireflection coating theory. The substrate was coated on both sides as described.

The layers of optical coatings were prepared by using electron beam evaporation and thermal evaporation techniques at room temperature. The evaporation source was a MRC electron beam evaporator with a four-crucible rotating source. The layer thickness control was achieved with an Inficon quartz crystal monitor. The electron beam current was 15 mA for MgO at an acceleration voltage of 3 kV, resulting in a deposition rate of 1.5 Å/s. MgF_2 is deposited on MgO films by using the thermal evaporation method by a deposition rate of 2.0 Å/s. The peak transmittance of double layer coating is 98.2% at $\lambda_0 = 450$ nm, as shown in Figure 4. Experimental and theoretical curves of this coating show very good agreement. The small difference between experimental and theoretical curves is believed to be caused by the refractive index variation.

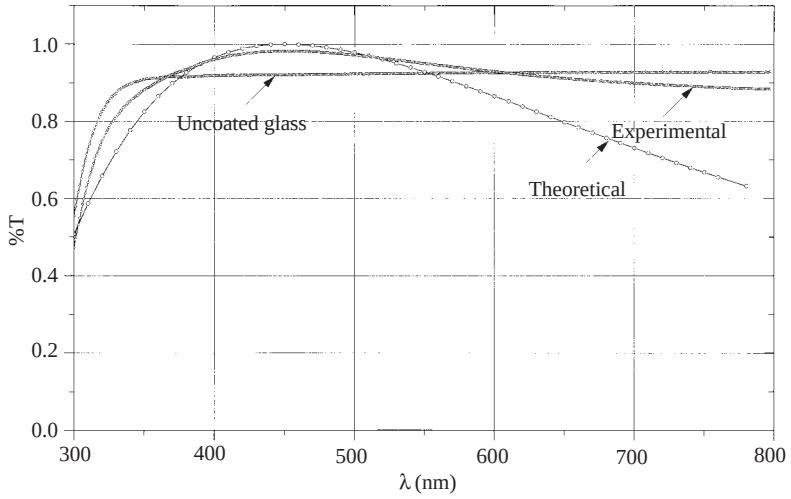

Figure 4. Transmittance of a double layer MgO/MgF_2 antireflection coating deposited on glass substrates for a central wavelength of 450 nm. Curves of theory, experiment and bare glass are shown for comparison.

4. Conclusion

In this article, we have presented the optical matrix approach method to design and obtain theoretical transmittance and reflectance values of optical coatings. This method directly calculates the theoretical optical transmittance and reflectance values of optical coatings by using only refractive indexes and physical thicknesses of coating materials. While calculating theoretical transmittance and reflectance values, no adjustable parameters were used. All obtained equations are exact solutions. Thus, when calculating transmittance and reflectance, it is a very useful and powerful method compared to other methods.

The transmittance and reflectance of various designs were calculated and plotted by using a small computer. The transmittance of prepared two-layer design, which consisted of MgO/MgF_2 on both sides of the glass substrate, was calculated and plotted. Experimental and theoretical curves of this coating show very good agreement.

References

[1] Introduction to Modern Optics, Grant R. Fowles, Holt Richard and Winston, Inc., New York, 1968.

[2] Thin Film Device Applications, Kasturi Lal Chopra, Inderjeet Kaur, Plenium Press, New York, 1983.

[3] H. A. Macleod, Thin-Film Optical Filters, Adam Hilger, Bristol, 1986.

[4] Handbook of Infrared Optical Materials, Paul Klocek, Marcel Dekker, Inc., New York, 1991.

[5] Introduction to Optics, Frank L. Pedrotti, S.J. Leno S. Pedrotti, Prentice-Hall, Inc., New Jersey, 1993.

[6] Thin Films for Optical Systems, Francois R. Flory, Marcel Dekker, Inc., Newyork, 1995.

[7] D. Pekker, L. Pekker, Thin Solid Films, **425**, (2003), 203

[8] P. Nubile, *Thin Solid Films*, **342**, (1999), 257.

[9] V.M. Aroutiounian, K.R. Maroutyan, A.L. Zatikyan, K.J. Touryan, *Thin Solid Films,* **403–404**, (2002), 517.

[10] H.G. Shanbhogue, C.L. Nagendra, M.N. Annapurna, S.A. Kumar, *App. Opt.* **36**, (1997), 6339.

[11] J.A. Dobrowolski, A.V. Tikhonravov, M.K. Trubetskov, B.T. Sullivan and P.G. Verly, *App. Opt.*, **35**, (1996), 644.

[12] J. Lee, T. Tanaka, S. Sasaki, S. Uchiyama, *Journal of Lightwave Technology* **16**, (1998), 884.

[13] Y. Zheng, K. Kikuchi, M. Yamasaki, K. Sonoi and K. Uehara, *App. Opt.* **36**, (1997), 6335.

[14] H. Niederwald, Thin Solid Films, **377–378**, (2000), 21.